RSC Advances

ROYAL SOCIETY OF CHEMISTRY

www.rsc.org/advances

Journal Name

RSCPublishing

ARTICLE

Ascorbic acid-coated Fe_3O_4 nanoparticles as a novel heterogeneous catalyst of persulfate for improving the degradation of 2,4-dichlorophenol

Cite this: DOI: 10.1039/xoxxoooooox

Received ooth January 2012,
Accepted ooth January 2012

DOI: 10.1039/xoxxoooooox

www.rsc.org/

Chao Sun,[a] Rui Zhou,[a,b] Jianan E,[a] Jiaqiang Sun,[a] Yu Su [a] and Hejun Ren[a]*

Magnetic nanoscaled ascorbic acid/magnetite (H_2A/Fe_3O_4) composite was prepared by oxidative polymerization and proposed as a novel heterogeneous catalyst of persulfate (PS) for improved degradation of 2,4-dichlorophenol (2,4-DCP). The composite was fully characterized and evaluated in terms of catalytic activity, effect of reaction parameters, iron ion leaching, and identification of primary reaction oxidants, as well as the possible role of H_2A. The degradation efficiency of 2,4-DCP reached 98.5% within 150 min using the H_2A/Fe_3O_4 nanocomposite compared with only 35.1% under the same conditions for pure nano Fe_3O_4. This result indicated an enhancement in the performance of activated PS. The findings of this study provide some new insights into the potential of using the H_2A to enhance the performance of Fe_3O_4 nanoparticles on the activation of PS for improving the degradation of organic pollutants.

Introduction

Advanced oxidation processes (AOPs) have gained popularity in recent years as an alternative for in situ oxidation of organic pollutants[1-3]. In particular, sulfate radical ($SO_4^{\bullet-}$)-based AOPs have received extensive research attention because of their excellent solubility, stable structure, relatively long half-life of $SO_4^{\bullet-}$ [2, 4], and high standard redox potential ($E^0 = 2.6$ V)[5, 6]. For $SO_4^{\bullet-}$ generation, the activation of persulfate (PS) by ultraviolet (UV)[7-9], heat[10], and transition metal ions (e.g., iron oxide[11-13] or zero valent iron[14, 15]) has been widely studied. Using Fe(II) or Co(II) has been found to be inexpensive and practical. However, at acidic pH values of pH 2–3, the accumulation of iron sludge and the potential health hazards limit the application of this homogeneous system[16, 17]. Considering these shortcomings, researchers diverted their attention to develop heterogeneous catalysts in a Fenton-like system.

Recently, Fe_3O_4 magnetic nanoparticles (MNPs) have attracted significant interest because they can work in mild conditions and facile recovery. Many studies have demonstrated that Fe_3O_4 nanoparticles can activate PS to degrade organic contaminants, which can be attributed to the initiation of the reaction by the presence of Fe(II) species in the magnetite structure. Unfortunately, the activation of PS by Fe_3O_4 nanoparticles does not show favorable catalytic performance[16, 18, 19], which may be due to the slow transformation from Fe(III) to Fe(II). Therefore, accelerating the redox cycle of Fe(III)/Fe(II) is necessary to improve the catalytic performance of Fe_3O_4 MNPs. As a result, increasing attention has been paid to development of a heterogeneous catalytic system by modifying surfaces of Fe_3O_4 MNPs with polymers. Some attempts have been reported, including polyhydroquinone-coated Fe_3O_4[20], humid acid modified Fe_3O_4[21], horseradish peroxidase modified magnetic Fe_3O_4/SiO_2 particles[22] and poly(3,4-ethlene-dioxythiophene) immobilized Fe_3O_4 [23] as catalysts for the activation of PS or H_2O_2. However, the cost-prohibitive or insufficient catalytic activity presents difficulties for their use in practical applications. Another possible approach for improving the catalytic performance of Fe_3O_4 MNPs may be the addition of an organic agent with a strong chelating or reducing ability. Wang et al.[24] found that EDTA

[a] *Key Laboratory of Groundwater Resources and Environment of the Ministry of Education, College of Environment and Resources, Jilin University, 2519 Jiefang Road, Changchun, 130021, P. R. China. Tel: +86-431-88502606; Email: renhejun@jlu.edu.cn*

[b] *Earth Sciences Division, Lawrence Berkeley National Laboratory, Berkeley, CA94720, United States*

† Electronic Supplementary Information (ESI) associated with this article including Text S1, Figures S1−S3 and Table S1 is available.

was one of the best organic chelating compounds and clarified that the enhancing effect of EDTA was attributed to an appreciable improvement of Fe^{3+}/Fe^{2+} recycling on the surface of Fe_3O_4 nanoparticles. However, metal–EDTA complexes are soluble and poorly biodegradable in water environment. This may cause serious pollution in different regions by the flow of water [25,26] and has a negative influence on ecosystems and health[27]. Given the facts above, it motivated us to develop an alternative means of improving the catalytic ability of Fe_3O_4 MNPs.

Ascorbic acid ($C_6H_8O_6$, H_2A), also called vitamin C, has been commonly considered as an antioxidant for its strong reducing property against reactive oxidants[28,29]. In recent years, H_2A has been tested as a redox mediator in wastewater treatment. Fukuchi et al. [30]and Lei et al. [31]reported that H_2A introduced into traditional Fenton-like processes (Fe^{2+}/PS or Fe^{2+}/H_2O_2) enhanced the removal efficiency of organic contaminants. Hence,we reasonably speculated that H_2A-modified Fe_3O_4 MNPs may enhance the performance of activated PS, but this theory remains untested to the best of our knowledge.

2,4-Dichlorophenol (2,4-DCP) is a derivative of phenol and a significantly harmful environmental contaminant that has high toxicity, recalcitrance, bioaccumulation, and persistence in the environment[32,33]. Given its toxicity to human health, it has been listed as a priority pollutant by the US EPA and the EU[34,35]. The present study aimed to explore the application of H_2A/Fe_3O_4 activator as a source to enhance the decomposition of PS and degrade organic pollutants. An efficient oxidation process was developed to degrade 2,4-DCP, and the activation mechanism of PS was clarified.

Materials and Methods

Reagents

Ferrous sulfate ($FeSO_4 \cdot 7H_2O$, 99%), ferric chloride ($FeCl_3 \cdot 6H_2O$, 99%), and ammonia water ($NH_3 \cdot H_2O$, 25%–28%) for the preparation of Fe_3O_4 MNPs were of analytical grade and purchased from Sinopharm Chemical Reagent Co., Ltd. 2,4-DCP (99%) was obtained from Sigma–Aldrich. All other chemicals, including sodium hydroxide (NaOH, 99%) and sulfuric acid (H_2SO_4, 95% to 98%), were of analytical grade and obtained from Tianjin, China. Sodium persulfate ($Na_2S_2O_8$) and ascorbic acid (H_2A) were supplied by Aladdin. Water purified using a Milli-Q system was used in all experiments.

Preparation and characterization of H_2A/Fe_3O_4

Fe_3O_4 MNPs were synthesized without a surfactant using previously reported methods [19, 36]. In brief, $FeSO_4 \cdot 7H_2O$ (2.78 g) and $FeCl_3 \cdot 6H_2O$ (2.705 g) were dissolved in 20 mL of deoxygenated water in an ultrasonic bath at 70 °C. The warm solutions were mixed and added dropwise to 40 mL of ammonia water (ammonia:water = 1:3). After black deposits were synthesized, MNPs were dispersed in an ultrasonic bath (frequency 40 kHz) for 60 min. The resulting precipitate was gradually cooled to room temperature. All procedures were conducted under nitrogen gas. The morphology and size distribution of pure Fe_3O_4 surveyed by transmission electronic microscopy (TEM) are shown in Supporting Information Figure S1.

H_2A/Fe_3O_4 MNPs were prepared through oxidative polymerization of H_2A as follows: 2.32 g of Fe_3O_4 was dispersed into 100 mL of deoxygenated water. An appropriate amount of H_2A based on the Fe_3O_4/H_2A mass ratio of 2.6:1 was added to the suspension solution above. After mixing for a certain period, 6 mL of $FeSO_4 \cdot 7H_2O$ solution (0.02 wt %) and 3.4 mL of H_2O_2 were added dropwise in 1 h. The mixture was then stirred for 24 h[29]. Finally, the solid product was collected using a magnet, washed with deionized water, and dried in a vacuum oven at 60 °C.

Experimental procedure

Stock solutions of 2,4-DCP (400 mg/L) and PS (300 mmol/L) were prepared using deionized water. Batch experiments were conducted in 100 mL serum bottles containing 30 mL of the reaction solution. The bottles were immersed in a shaking water bath at 150 rpm. The reaction was immediately initiated by adding the desired PS. Aliquots of 0.2 mL were obtained at given time intervals, quenched with excess pure methanol (0.2 mL)[37], and centrifuged for subsequent analysis. Each degradation test was performed in triplicate, and the average experimental values were reported.

Sample analysis

The degradation of 2,4-DCP was followed by analysis of test samples using high-performance liquid chromatography (HPLC, Agilent 1100, USA), equipped with a UV detector at 224 nm. A reversed-phase Agilent-C18 column (150 mm × 4.6 mm, 5 μm inner diameter) was utilized for HPLC analysis. The mobile phase was methanol and water in 0.02% acetic acid delivered in the ratio 70:30 (v/v). The mobile phase flow rate was fixed at 1 mL/min, and the run

time was 5.0 min. The concentrations of ferrous ions and total dissolved iron were measured colorimetrically with 1,10-phenanthroline through the absorption intensity at λ_{max} = 510 nm with a UV-visible spectrophotometer (Evolution 201, Thermo Scientific). Detailed procedures of iron determination were shown in Supporting Information Text S1.

Electron paramagnetic resonance (EPR) with 5,5-dimethyl-1-pyrroline N-oxide (DMPO) as a spin-trapping agent was used to characterize the generation of radicals, and its detailed parameters and procedures are given in Supporting Information Text S2.

Results and discussion

Characterization of catalysts

Figure 1a shows the X-ray diffraction patterns of Fe_3O_4 and H_2A/Fe_3O_4. Within the range of 10° to 70°, a series of characteristic peaks was present, with some positions matching well with those in the JCPDs card (NO. 19-0629) of Fe_3O_4 and H_2A/Fe_3O_4.

As shown in Figure 1b, the nitrogen adsorption–desorption isotherms exhibited typical type IV characteristics according to the Brunauer–Deming–Deming–Teller classification, which indicated that the Fe_3O_4/H_2A composite was typical of a mesoporous structure[38]. The Brunauer–Emmett–Teller surface area, pore volume, and pore diameter of Fe_3O_4/H_2A determined from the N_2 adsorption–desorption isotherms were 108.31m^2g^{-1}, 0.22 cm^3 g^{-1}, and 8.20 nm, respectively.

The high-resolution TEM image in Figure 1c shows regular and uniform particles with a diameter of 10–20 nm. The lattice fringe spacing of the composite was approximately 0.25 nm, which could be assigned to the (311) reflection of Fe_3O_4. Fourier-transform infrared spectra were determined in the frequency range 400–4000 cm^{-1}, in which the absorptions at 1113 cm^{-1}, 1316 cm^{-1}, and 1360 cm^{-1} (also found in the H_2A spectrum shown in SI Figure S2 and SI Table S1) were related to C–O groups. Meanwhile, an additional band around 1628 cm^{-1} could be attributed to the stretching vibrations of C = C groups, indicating the presence of the H_2A constituent. The magnetic properties of the as-synthesized samples were determined at room temperature (Supporting Information Figure S3). The results further confirmed that the composite could be collected by an external magnetic field and then reused, which is one of the advantages of this prepared material.

Catalytic activity of H_2A/Fe_3O_4

Comparative experiments were carried out in different systems to determine the effects of the synthesized H_2A/Fe_3O_4 composites on PS activation for 2,4-DCP degradation. These experiments were conducted in the same reactor and controlled under the same operating conditions. The results are shown in Figure 2. Nearly no 2,4-DCP was removed with PS alone, indicating that PS had no reactivity without the presence of activators. A similar phenomenon was observed in the H_2A–PS system. Low 2,4-DCP degradation was noted (7.5%), suggesting that the production of oxidizing radicals from PS could not occur without catalysts. To verify whether modification of H_2A enhances the performance of Fe_3O_4 in activating PS, experiments were conducted with 2 g/L H_2A/Fe_3O_4. The performance was compared with those of 2 g/L Fe_3O_4 and 30 mmol/L PS in the presence of 100 mg/L 2,4-DCP. Figure 2 shows that only 35.1% 2,4-DCP could be removed from the solution by Fe_3O_4 with PS. Remarkably, a significant decrease in the 2,4-DCP concentration was observed once Fe_3O_4/H_2A was added, and an evidently improved 2,4-DCP removal efficiency of 63.4% was achieved in the H_2A/Fe_3O_4 system with 30 mmol/L PS and a reaction time of 150 min. The results in Figure 2 also show that PS only led to a slight removal of 2,4-DCP within 150 min, and the small amounts of 2,4-DCP eliminated by H_2A/Fe_3O_4 and Fe_3O_4 were primarily ascribed to the surface adsorption of these two kinds of materials, which was negligible compared with the rapid removal of 2,4-DCP by heterogeneous PS-activated reaction. Moreover, when Fe_3O_4 and free H_2A were both activators for PS, the degradation efficiency was lower than that of H_2A/Fe_3O_4 and higher than that of Fe_3O_4. We infer the reason is that free H_2A is difficult to contact with Fe (III) on the surface of Fe_3O_4, resulting in the lower efficiency of reducing Fe (III) on the surface of Fe_3O_4 than after polymerization. So it showed that the degradation efficiency of 2,4-DCP by PS + H_2A/Fe_3O_4 is much better than that by PS + H_2A + Fe_3O_4. In order to confirm this point, we recorded the FTIR sepctra (Supporting Information Figure S4) of Fe_3O_4 powders before and after the immersion treatment in H_2A solution referred to the reports of Wang et al [39]. The results showed that there are no remarkable peaks in Fe_3O_4 after absorption at 1316 cm^{-1} and 1360 cm^{-1} which represents the C–O groups for H_2A. It means that free H_2A weakly adsorbed on the surface of Fe_3O_4.

Factors influencing 2,4-DCP degradation

Figure 3a shows the effect of the Fe_3O_4/H_2A dosage on 2,4-DCP degradation by PS activation. As observed, the increase in the activator dosage from 0.5 g/L to 2.0 g/L promoted the degradation of 2,4-DCP, which could be attributed to the higher production of reactive free radicals by PS activation. At a lower dosage of Fe_3O_4/H_2A (2.0 g/L), 98.5% removal could be obtained within 150 min, indicating excellent activity of Fe_3O_4/H_2A for PS activation to 100 mg/L 2,4-DCP. The removal efficiency of 2,4-DCP did not improve when the H_2A/Fe_3O_4 dosage reached 2.5 g/L. Considering economic cost and usability, 2.0 g/L was more practical to use than 2.5 g/L. Our findings were similar to previous observations for PS/PHQ/Fe_3O_4 degrading Rhodamine B at 0.02 mM [20].

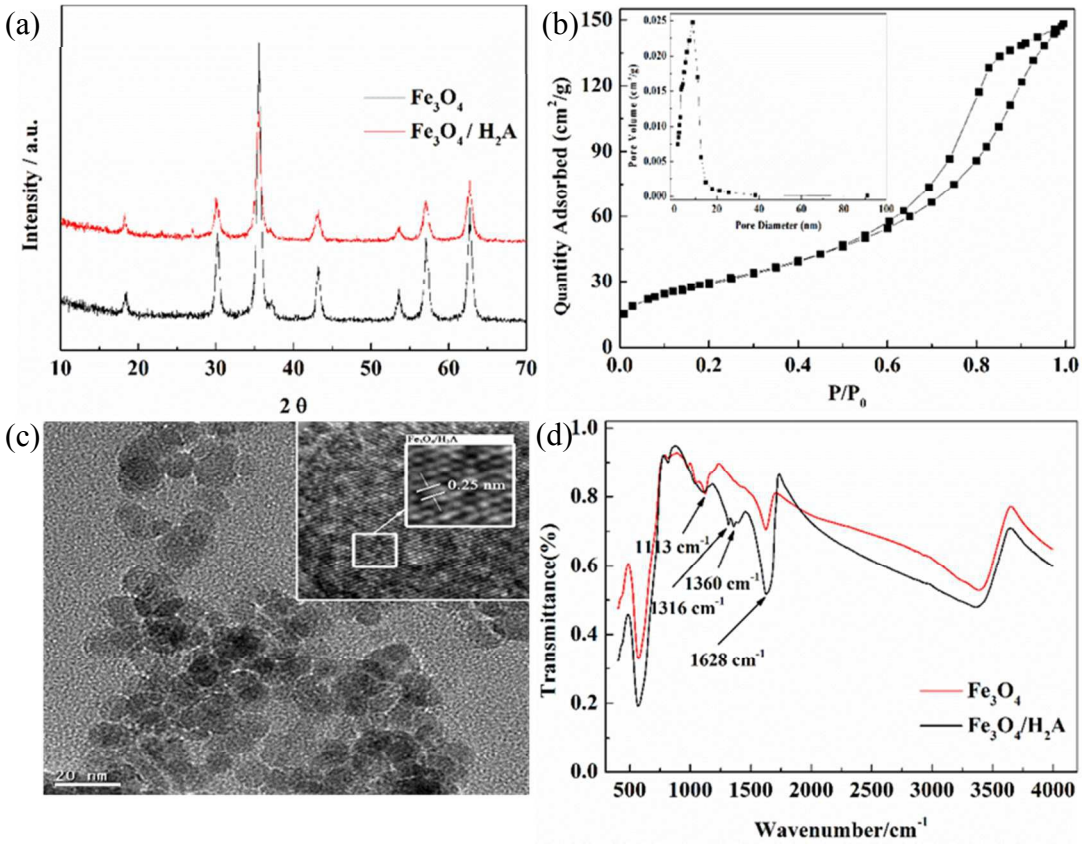

Figure 1. Characterization of catalysts. (a) X-ray diffraction pattern. (b) Nitrogen absorption/desorption isotherms and pore size distribution curve (inset). (c) High-resolution transmission electron microscopy images. (d) Fourier-transform infrared spectra of Fe_3O_4 and H_2A/Fe_3O_4.

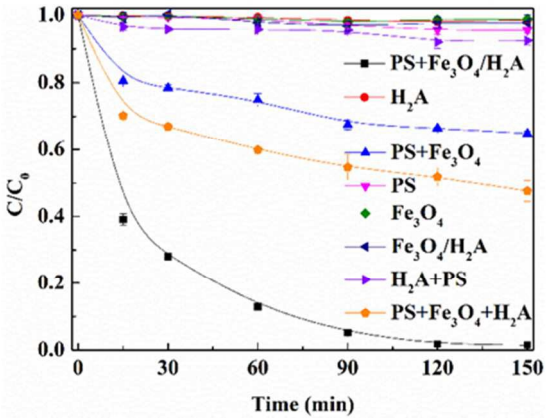

Figure 2. Degradation efficiency of 2,4-DCP in different systems. Conditions: [PS] = 30.0 mM; [Fe_3O_4] = 2.0 g/L; [H_2A] = 2.0 g/L; [H_2A/Fe_3O_4] = 2.0 g/L; [2,4-DCP] = 100 mg/L.

As the driving force of the formation of SO_4^{-}• and •OH, PS played an important role in the degradation of 2,4-DCP. In the presence of H_2A/Fe_3O_4 alone, only 2.3% removal was observed within 150 min from Figure 3b. When PS was added to the solution, significant degradation efficiency was observed. At a fixed dosage of activators at 2.0 g/L, the variation in PS dosage from 10 mmol/L to

30 mmol/L resulted in an increase in the efficiency of 2,4-DCP degradation from 94.8% to 98.5% within 150 min. However, at excess PS concentrations, such as 40 and 50 mmol/L PS, the generated sulfate radicals would be consumed, leading to the decline in the 2,4-DCP degradation efficiency in keeping with previous studies[18, 40]. Hence, 30 mM PS was selected as the optimal PS dosage for subsequent experiments.

As the solution pH can remarkably influence the oxidative degradation of organic pollutants, the effects of this parameter in the system were explored by varying pH within the range of 3.0 ± 0.3 to 11.0 ± 0.3, and the results are presented in Figure 3c. The highest degradation efficiency was observed at pH 3.0 ± 0.3, and the degradation rate decreased with the increase in pH from pH 3.0 ± 0.3 to pH 9.0 ± 0.3 in agreement with Leng's work [20]. However, when the initial pH reached pH 11.0 ± 0.3, a degradation efficiency greater

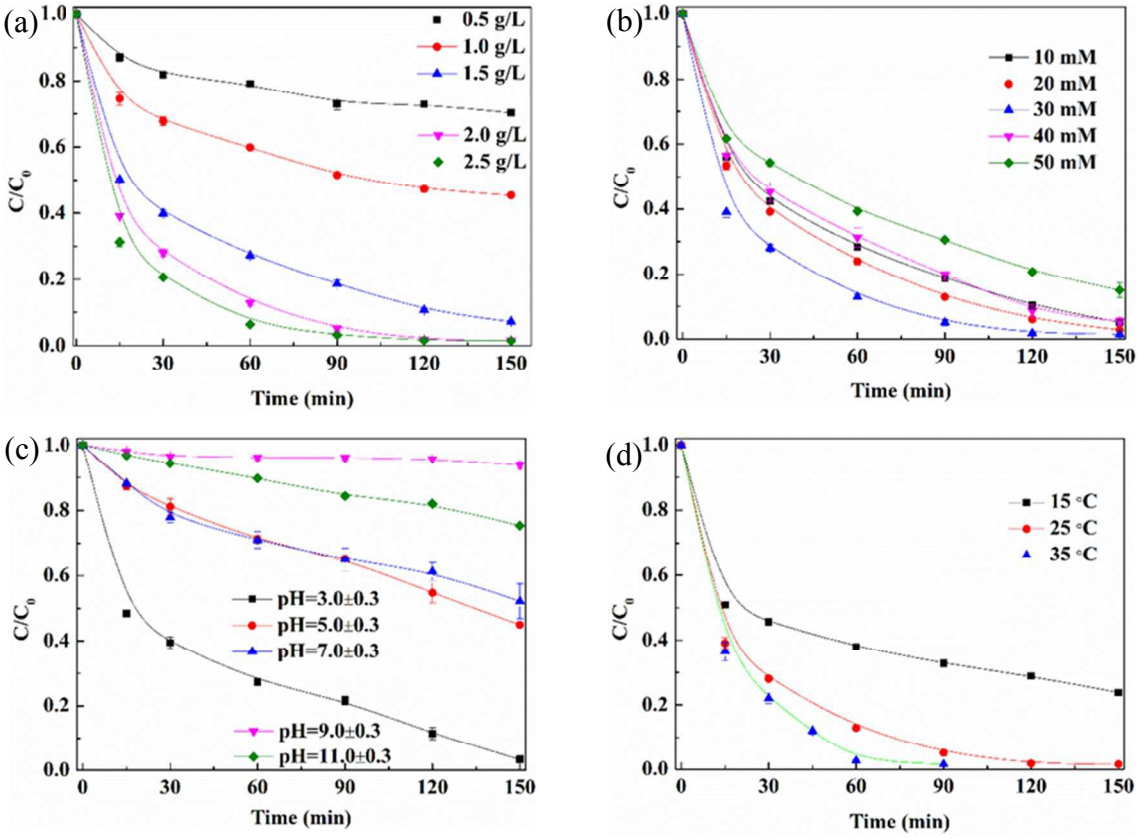

Figure 3. Influence of different initial parameters on 2,4-DCP degradation in the activation of PS catalyzed by H_2A/Fe_3O_4: (a) H_2A/ Fe_3O_4 addition, (b) PS dosage, (c) pH, and (d) temperature. Except for the investigated parameter, other parameters were fixed at PS = 30.0 mM, H_2A/Fe_3O_4 = 2.0 g/L, 2,4-DCP = 100 mg/L, and temperature = 25 °C.

than that at pH 9.0 ± 0.3 was observed. This finding may be because PS was simultaneously activated both under alkaline conditions [41,42] and with H_2A/Fe_3O_4.

Figure 3d illustrates the effect of temperature (15 °C, 25 °C, and 35 °C) on the degradation of 2,4-DCP by PS activated with H_2A/Fe_3O_4, with activator and PS dosages of 2.0 g/L and 30 mmol/L, respectively. Higher temperatures favored the degradation of 2,4-DCP by PS activated with H_2A/Fe_3O_4, which could be associated with the thermal activation of PS to generate free radicals[10, 43] and the acceleration of the reaction between H_2A/Fe_3O_4 and PS. In accordance with Arrhenius kinetics, increasing the temperature increased the degradation rate. However, elevating the temperature was troublesome to be implemented in real applications. Thus, the experiments were carried out at room temperature (25 °C) in the following work.

Iron dissolution during 2,4-DCP degradation

The concentrations of ferrous and dissolved iron in the solution were determined during the oxidation of 2,4-DCP adopted as standard reaction conditions. As shown in Figure 4, the concentration of ferrous ion increased first and then decreased in the last 90 min of the reaction. Thus, the ferrous concentration peaked at 60 min when 87.1% 2,4-DCP was removed. Subsequently, the ferrous concentration decreased to 2.3 mg/L at 90 min of reaction, corresponding to low degradation efficiency (7.8%) from the 60th minute to the 90th minute. The degradation rate in the period when more ferrous ions were released by the oxidation of catalyst with PS was faster than the last 90 min of the reaction. As previously reported, the decrease in the ferrous ion concentration may be caused by the oxidation of ferrous ions into ferric ions by the remaining oxidants, such as PS and excess free radicals, in the solution. Nevertheless, the concentration of total dissolved iron increased as the reaction time increased with no descending period, which could be attributed to the continuous leaching of iron from H_2A/Fe_3O_4. The highest loss of iron amounted to 42.6 mg/L, equivalent to approximately 4.06% of total iron of 2.0 g/L H_2A/Fe_3O_4 catalyst used. By comparison, the leaching of iron was faster during 2,4-DCP degradation by H_2A/Fe_3O_4 composite than pure Fe_3O_4 in a previously reported Fenton-like reaction[44]. However, according to the preparation method, the H_2A/Fe_3O_4 was finally treated by $FeSO_4$ + H_2O_2 (Fe^{2+} is equal to 0.42% of Fe(II)), which may be closely related to the enhancement of Fe dissolution of H_2A/Fe_3O_4. To confirm this possibility, the SEM and the measurement of total iron were used to detect any changes in the surface morphology and composition of Fe_3O_4 MNPs by the $FeSO_4$ + H_2O_2 treatment. The results indicated the surface morphology had not obviously changed after treatment (as shown in Supporting Information Figure S5). And the total iron of Fe_3O_4 after the $FeSO_4$ + H_2O_2 treatment is equal to the unprocessed object, using 1,10-phenanthroline colorimetry at λmax = 510 nm with a UV-visible spectrophotometer (Evolution 201, Thermo Scientific) [16,44,45]. These results implied that the H_2A has important role in the redox cycling of Fe.

Identification of primary reactive oxidants

Reactive oxidants, such as $SO_4^{\bullet-}$ and •OH, are commonly considered as possible radicals in the catalyst-mediated decomposition of PS. To identify the reactive species mediated in the H_2A/Fe_3O_4/PS process, several quenching tests were carried out using methanol and *tert*-butyl alcohol (TBA) as radical scavengers in 2,4-DCP degradation. Methanol is an effective quencher for both $SO_4^{\bullet-}$ ($k=2.5\times10^7\ M^{-1}s^{-1}$) [46] and •OH ($k=9.7\times10^8\ M^{-1}s^{-1}$) [47], whereas TBA mainly reacts with •OH ($k=6.0\times10^8\ M^{-1}s^{-1}$) [46] and is not effective for $SO_4^{\bullet-}$ ($8.0\times10^5\ M^{-1}s^{-1}$) [47].

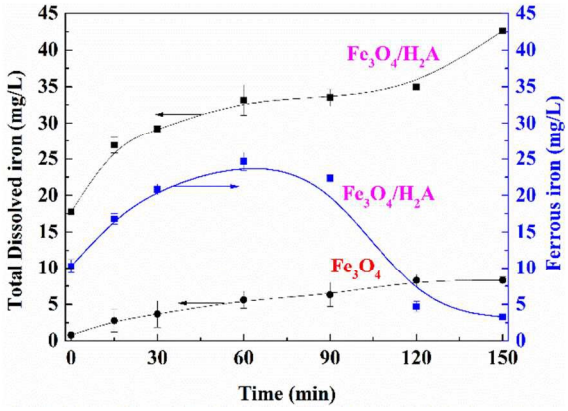

Figure 4. Analysis of iron dissolution during 2,4-DCP degradation with 30.0 mM PS, 2.0 g/L H_2A/Fe_3O_4 or 2.0g/L Fe_3O_4 , 100 mg/L 2,4-DCP, and temperature of 25°C.

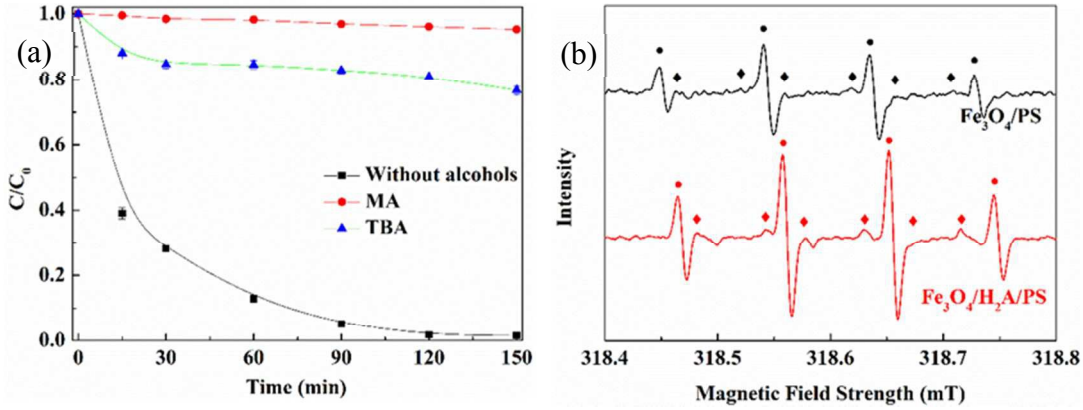

Figure 5. (a) Effect of radical scavengers on the degradation of 2,4-DCP. (b) Electron paramagnetic resonance spectra of PS and the catalysts

in the presence of 0.1 M DMPO (● represents •OH adduct, and ◆ represents $SO_4^{\bullet-}$ adduct).

As shown in Figure 5a, the degradation efficiency of 2,4-DCP decreased from 98.5% to 23.3% during a reaction time of 150 min with the addition of excess TBA (2.5 M). Meanwhile, the addition of 10 M methanol almost completely inhibited the degradation of 2,4-DCP, which meant that both $SO_4^{\bullet-}$ and •OH were the primary oxidative free radical species responsible for 2,4-DCP degradation. To verify the absence of •OH and $SO_4^{\bullet-}$ in the H_2A/Fe_3O_4/PS process, EPR experiments were performed to identify these radicals by adding the spin-trapping agent DMPO. In Figure 5b, the fourfold characteristic peak with an intensity ratio of 1:2:2:1 in accordance with those of DMPO–OH adducts [48] and the pattern of typical DMPO–SO_4 adducts [49] were shown in the EPR spectra of Fe_3O_4 and H_2A/Fe_3O_4/PS systems, respectively. The intensity of DMPO radical adduct signals in the H_2A/Fe_3O_4/PS process was much stronger than that in the Fe_3O_4/PS process. These results further confirmed that both $SO_4^{\bullet-}$ and •OH were generated in the H_2A/Fe_3O_4/PS process, and H_2A-modified Fe_3O_4 accelerated the generation of reactive oxidants.

Possible role of H_2A in H_2A/Fe_3O_4/PS

In the similar Fe-containing systems for oxidative decomposition of organic pollutants by using persulfate, J. Yan et al[50] pointed out that the highly efficient activation effect of the ferrous hydroxide colloids was attributed to the intrinsic nature of colloid particles with large specific surface area, which simultaneously increased the chemical attack possibility of persulfate and the adsorption of organic pollutants on the colloidal surface. Our data also clearly demonstrated that H_2A/Fe_3O_4 exhibited superior activity in the activation of PS for 2,4-DCP than pure Fe_3O_4. However, considering that the aggregation of catalyst coated with H_2A in the solution was still remarkable (Figure 1c), we believe that the high catalytic ability of H_2A/Fe_3O_4 did not mainly result from the increased dispersibility in solution. A previous study reported that H_2A can perform a major role as a chelating and reducing agent [31], and the release of metal ions from minerals can be enhanced by chelating agents [51].

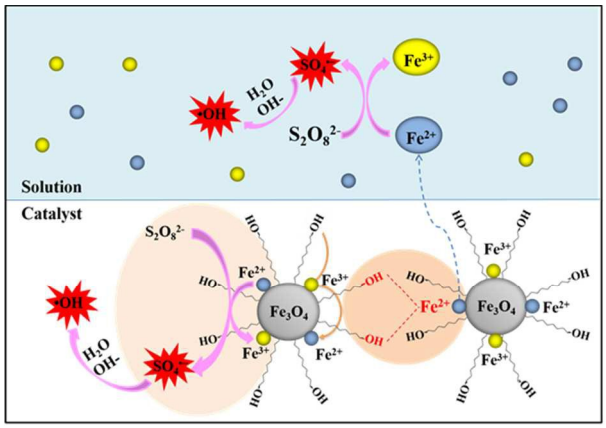

Figure 6. Possible mechanism of enhanced 2,4-DCP degradation in the H_2A/Fe_3O_4 /PS process.

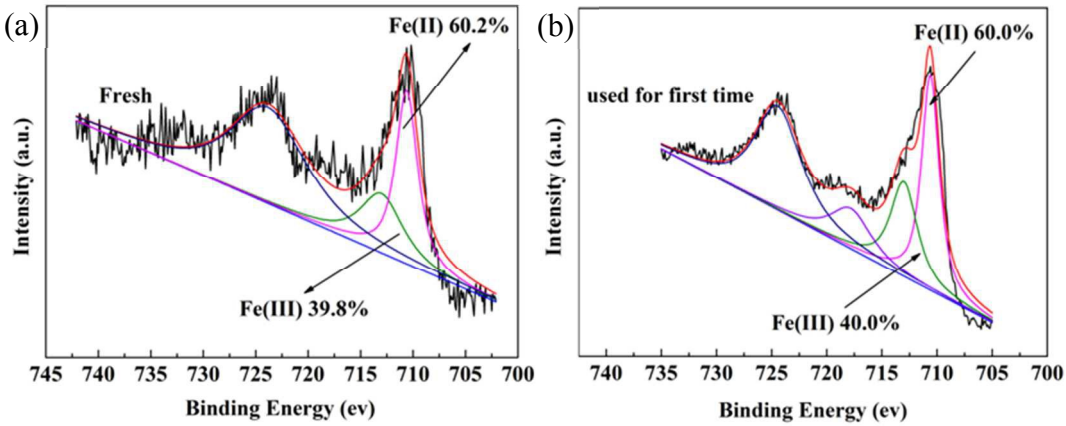

Figure 7. (a) X-ray photoelectron spectra for Fe 2p regions of fresh (b) X-ray photoelectron spectra for Fe 2p regions of used H_2A/Fe_3O_4 for first time.

The primary mechanism of enhanced 2,4-DCP degradation by the H_2A/Fe_3O_4/PS process is proposed in Figure 6, showing that H_2A affected both the surface and aqueous reactions. First, H_2A coated on the Fe_3O_4 particles acts as a chelating agent on Fe^{2+}, which forms Fe^{II}–H_2A surface complexes on the surface of other particles via the ligand exchange reaction. Fe^{2+} can then be released from the surface into the aqueous phase, resulting in the increase in the total dissolved irons dissolved irons and ferrous ions in the solution, thereby enhancing the homogeneous Fenton-like reaction. These inferences were consistent with our experiments, as shown in Figure 4. In the H_2A/Fe_3O_4/PS process, the highest amount of dissolved iron was 42.6 mg/L, and the highest amount of Fe^{2+} was 22.5 mg/L. By contrast, using pure Fe_3O_4 resulted in only 8.3 mg/L total dissolved iron and ferrous ion was below the detection limit.

In addition, H_2A can as a reducing agent improved the reduction of Fe(III) to Fe(II) on the surface and enhanced the heterogeneous Fenton-like reaction on the Fe_3O_4 nanoparticle surface. To verify this speculation, surface structure information of H_2A/Fe_3O_4 was analyzed by X-ray photoelectron spectroscopy before and after 2,4-DCP degradation (Figure 7). Regarding the fresh catalyst, the high-resolution spectra of the peaks at 710.6 and 713.0 eV were indicative of the presence of Fe(II) and Fe(III)[17]. After the reaction, the proportion of Fe(II) species declined slightly from 60.2% to 60.0%. These results confirmed that the reduction of Fe(III) to Fe(II) on the surface by H_2A occurred. The effect of H_2A favorable for the Fe(III) to Fe(II) cycle has similarity with that of EDTA reported in the work of M. Wang[24] and N. Wang[39]. However, the mechanisms of promoting this cycle are different. As proposed in their reports, the complex of Fe^{3+}/Fe^{2+} with EDTA decreased the Fe^{3+}/Fe^{2+} redox potential from 0.77 V to 0.209 V, enhancing the thermodynamic driving force for the Fenton reaction. In addition, the reduction rate constant of Fe^{3+} with O_2^{-}•/HO_2• increased from 1.4 (or 3.5) x 10^5 M^{-1} s^{-1} in the absence of EDTA to 2 x10^6 M^{-1} s^{-1} in the presence of EDTA. Whereas, our data confirmed that the H_2A itself as a reducing agent could directly convert Fe(III) into Fe(II), which was supported by the report of Lei et al[31].

Recently, Jia Huang, et al[52] observed that the simultaneously using of HRP and GO/Fe_3O_4 yielded a removal of 2,4-DCP as high as 93% in the presence of H_2O_2. And the research proposed that the removal mechanism of 2,4-DCP was attributed to the production of insoluble polymers. However, in our reaction system, we didn't find the formation of insoluble polymers, which is consistent with the report by Jingchun Yan et al.[40]. The reason may be the oxidant we took is PS rather than H_2O_2 and the life time of sulfate radicals are longer than hydroxyl radicals[53]. The essential difference in final reaction products hinting that if comprehensively clarifying the degradation mechanism of 2,4-DCP in our tested system，we must recognize some problems including the intermediate products of 2,4-DCP degradation, the fate of H_2A, whether the intermediate products reaction with H_2A or not, and the contribution ratio between chelating and reducing functions of H_2A. But, these problems are quite complex and need to be investigated by target experiments in our further work.

Conclusion

This paper presents the successful fabrication of novel H_2A/Fe_3O_4 nanocomposites through a simple strategy and demonstrates the application of these nanocomposites as heterogeneous catalysts of PS for improving the degradation of 2,4-DCP. Investigations, including catalytic activity test, effect of reaction parameters, metal leaching, and identification of primary reaction oxidants, provide novel insights into the potential of using H_2A to enhance the performance of nano Fe_3O_4 on the activation of PS .The primary mechanism of the enhancement of 2,4-DCP degradation by the H_2A/Fe_3O_4/PS process is proposed, which attributed to the both chelating and reducing effects of H_2A. However, many aspects need to be further explained, such as the fate of H_2A and the degradation products of pollutants.

Acknowledgements

This work is financially supported by the National Natural Science Foundation of China (Grant No. 41302184), Scientific Frontier and Interdisciplinary Research Project of Jilin University, Outstanding Youth Cultivation Plan of Jilin University, Promotion of Innovation Ability of Beijing Municipal Universities Project by Beijing Municipal Education Commission (Grant No. TJSHG201310772028), and Graduate Innovation Fund of Jilin University (Grant No. 2015112). Key Laboratory of Groundwater Resources and Environment of Ministry of Education (Jilin University) is acknowledged for providing support to the work.

Notes and references

1. H. Liu, T.A. Bruton, F.M. Doyle and D.L. Sedlak, *Environ. Sci. Technol.*, 2014, **48**, 10330-10336.

2. G. Fang, J. Gao, D.D. Dionysiou, C. Liu and D. Zhou, *Environ. Sci. Technol.*, 2013, **47**, 4605-4611.
3. M. Xu, X. Gu, S. Lu, Z. Qiu, Q. Sui, Z. Miao, X. Zang and X. Wu, *J. Hazard. Mater.*, 2015, **286**, 7-14.
4. J. Yan, L. Han, W. Gao, S. Xue and M. Chen, *Bioresour. Technol.*, 2015, **175**, 269-274.
5. C. Liang, C.J. Bruell, M.C. Marley and K.L. Sperry, *Chemosphere.*, 2004, **55**, 1225-1233.
6. C. Liang, C.J. Bruell, M.C. Marley and K.L. Sperry, *Chemosphere.*, 2004, **55**, 1213-1223.
7. C.-W. Wang and C. Liang, *Chem. Eng. J.*, 2014, **254**, 472-478.
8. P. Xie, J. Ma, W. Liu, J. Zou, S. Yue, X. Li, M.R. Wiesner and J. Fang, *Water Res.*, 2015, **69**, 223-233.
9. W. Chu, D. Li, N. Gao, M.R. Templeton, C. Tan and Y. Gao, *Water Res.*, 2015, **72**, 340-348.
10. A. Ghauch, A.M. Tuqan and N. Kibbi, *Chem. Eng. J.*, 2015, **279**, 861-873.
11. G.-D. Fang, D.D. Dionysiou, S.R. Al-Abed and D.-M. Zhou, *Appl. Catal. B-Environ.*, 2013, **129**, 325-332.
12. S. Zhang, X. Zhao, H. Niu, Y. Shi, Y. Cai and G. Jiang, *J. Hazard. Mater.*, 2009, **167**, 560-566.
13. C. Tan, N. Gao, Y. Deng, J. Deng, S. Zhou, J. Li and X. Xin, *J. Hazard. Mater.*, 2014, **276**, 452-460.
14. C. Liang and Y.-y. Guo, *Environ. Sci. Technol.*, 2010, **44**, 8203-8208.
15. I. Hussain, Y. Zhang and S. Huang, *RSC Adv.*, 2014, **4**, 3502-3511.
16. L. Xu and J. Wang, *Environ. Sci. Technol.*, 2012, **46**, 10145-10153.
17. Y. Lei, C.S. Chen, Y.J. Tu, Y.H. Huang and H. Zhang, *Environ. Sci. Technol.*, 2015, **49**, 6838-6845.
18. R. Li, X. Jin, M. Megharaj, R. Naidu and Z. Chen, *Chem. Eng. J.*, 2015, **264**, 587-594.
19. C. Sun, R. Zhou, J. E, J. Sun and H. Ren, *RSC Adv*., 2015, **5**, 57058-57066.
20. Y. Leng, W. Guo, X. Shi, Y. Li and L. Xing, *Ind. Eng. Chem. Res.*, 2013, **52**, 13607-13612.
21. H. Niu, D. Zhang, S. Zhang, X. Zhang, Z. Meng and Y. Cai, *J. Hazard. Mater.*, 2011, **190**, 559-565.
22. Q. Chang and H. Tang, *Molecules*, 2014, **19**, 15768-15782
23. S. Shin, H. Yoon and J. Jang, *Catal. Commun.*, 2008, **10**, 178-182.
24. M. Wang, N. Wang, H. Tang, M. Cao, Y. She and L. Zhu, *Catal. Sci. Technol.*, 2012, **2**, 187-194.
25. J. Wang, X. Wang, G. Li, P. Guo and Z. Luo, *J. Hazard. Mater.*, 2010, **176**, 333-338.
26. X. Liu, J.-H. Fan, Y. Hao and L.-M. Ma, *Chem. Eng. J.*, 2014, **250**, 354-365.
27. L. T. Chen, T. Liu and C. A. Ma, *J. Phys. Chem. A*, 2010, **114**,443–454.
28. J. Feng, Y. Ju, J. Liu, H. Zhang and X. Chen, *Anal. Chim. Acta*., 2015, **854**, 153-160.
29. J.Y. Kim, M.J. Kim, B. Yi, S. Oh and J. Lee, *Food Chem.*, 2015, **176**, 302-307.
30. S. Fukuchi, R. Nishimoto, M. Fukushima and Q. Zhu, *Appl. Catal. B-Environ.*, 2014, **147**, 411-419.
31. Y. Lei, H. Zhang, J. Wang and J. Ai, *Chem. Eng. J.*, 2015, **270**, 73-79.
32. Z. Sun, X. Wei, Y. Han, S. Tong and X. Hu, *J. Hazard. Mater.*, 2013, **244-245**, 287-294.
33. H. Ren, Y. Zhan, X. Fang and D. Yu, *RSC Adv.*, 2014, **4**, 62631-62638.
34. M. Sathishkumar, A. Binupriya, D. Kavitha, R. Selvakumar, R. Jayabalan, J. Choi and S. Yun, *Chem. Eng. J.*, 2009, **147**, 265-271.
35. J. Pan, X. Zou, X. Wang, W. Guan, Y. Yan and J. Han, *Chem. Eng. J.*, 2010, **162**, 910-918.
36. Y.S. Zhao, C. Sun, J.Q. Sun and R. Zhou, *Sep. Purif. Technol*., 2015, **142**, 182-188.
37. L. Hou, H. Zhang and X. Xue, *Sep. Purif. Technol.*, 2012, **84**, 147-152.
38. M. Kruk and M. Jaroniec, *Chem. Mater.*, 2001, **13**, 3169-3183.
39. N. Wang, L. Zhu, M. Lei, Y. She, M. Cao and H. Tang, *ACS Catalysis*, 2011, **1**, 1193-1202.
40. J. Yan, M. Lei, L. Zhu, M.N. Anjum, J. Zou and H. Tang, *J. Hazard. Mater.*, 2011, **186**, 1398-1404.
41. O.S. Furman, A.L. Teel and R.J. Watts, *Environ. Sci. Technol.*, 2010, **44**, 6423-6428.
42. D. Zhao, X. Liao, X. Yan, S.G. Huling, T. Chai and H. Tao, *J. Hazard. Mater.*, 2013, **254-255**, 228-235.
43. M. Nie, Y. Yang, Z. Zhang, C. Yan, X. Wang, H. Li and W. Dong, *Chem. Eng. J.*, 2014, **246**, 373-382.
44. L. Xu and J. Wang, *Appl. Catal. B-Environ*., 2012, **123-124**, 117-126.
45. C. Lee, C. R. Keenan and D. L. Sedlak, *Environ. Sci. Technol*., 2008, **42**, 4921-4926.
46. P. Neta, R.E. Huie and A.B. Ross, *J. Phys. Chem. Ref. Data.*, 1988, **17**, 1027-1284.
47. G.V. Buxton, C.L. Greenstock, W.P. Helman and A.B. Ross, *J. Phys. Chem. Ref. Data.*, 1988, **17**, 513-886.
48. L. Chen, J. Ma, X. Li, J. Zhang, J. Fang, Y. Guan and P. Xie, *Environ. Sci. Technol.*, 2011, **45**, 3925-3930.
49. P.L. Zamora and F.A. Villamena, *J. Phys. Chem. A.*, 2012, **116**, 7210-7218.
50. J. Yan, L. Zhu, Z. Luo, Y. Huang, H. Tang and M. Chen, *Sep. Purif. Technol.*, 2013, **106**, 8-14.
51. B. Nowack, *Environ. Sci. Technol.*, 2002, **36**, 4009-4016.
52. J. Huang, Q. Chang, Y. Ding, X. Han and H. Tang, *Chem. Eng. J.*, 2014, **254**,434-442
53. A. Rastogi, S. R. Al-Abed and D. D. Dionysiou, *Appl. Catal. B-Environ.*, 2009, **85**, 171-179.

Graphical abstract